



## Effective adsorption of tetracycline by Fe-Mn-Ce composite metal oxides: kinetics, isotherm and mechanism

Bai Sun<sup>a,b</sup>, Menghao Sun<sup>a</sup>, Jie Zhang<sup>a</sup>, Fengshou Zhao<sup>a</sup>, Chenxu Shao<sup>a</sup>, Mingjian Yi<sup>a</sup>, Yun Wang<sup>a</sup>, Xiangxiang Wang<sup>a,\*</sup>, Shuguang Zhu<sup>a</sup>, Xinli Cai<sup>a</sup>

<sup>a</sup>Anhui Institute of Urban and Rural Green Development and Urban Renewal, College of Environment and Energy Engineering, Anhui Jianzhu University, Hefei 230601, China, Tel.: +86-551-63828252; Fax: +86-551-63828252; emails: 350992818@qq.com (X. Wang), bsun@mail.ustc.edu.cn (B. Sun), 1343695583@qq.com (M. Sun), 1045441563@qq.com (J. Zhang), 1132959870@qq.com (F. Zhao), 2624575993@qq.com (C. Shao), mjyi@ustc.edu.cn (M. Yi), 596820989@qq.com (Y. Wang), zhushuguang@ahjzu.edu.cn (S. Zhu), ahcxl@163.com (X. Cai)

<sup>b</sup>Environmental Materials and Pollution Control Laboratory, Hefei Institute of Physical Science, Chinese Academy of Sciences, Hefei 230031, China

Received 19 April 2023; Accepted 1 August 2023

### ABSTRACT

Fe-Mn-Ce metal oxides (FeMC) were prepared by using a co-precipitation method for the removal of tetracycline (TC). The FeMC composite has a good adsorption performance, and the maximum adsorption capacity at 318 K is 307.692 mg/g. FeMC metal oxides maintain good stability, and the removal rate of TC still reaches 85.24% after 5 cycles. The structural characteristics and adsorption mechanism of FeMC adsorbent have been systematically studied. According to the study of adsorption kinetics and adsorption isotherms, the adsorption process conforms to the quasi-second-order kinetic model. Langmuir isotherm model is more suitable than Freundlich isotherm model to describe the adsorption equilibrium data. The Fourier-transform infrared spectrum shows that the adsorption between FeMC and TC is realized by the stretching vibration of C–H and the stretching vibrations of C–O or C–O–C.

*Keywords:* Fe-Mn-Ce; Tetracycline; Adsorption; Nanocomposite

### 1. Introduction

In recent years, antibiotics have been used as drugs for treating diseases and aquaculture [1]. With widespread use, antibiotic residues accumulate in the environment. Since antibiotics cannot be metabolized by organisms, a large number of antibiotics enter water or soil through organic excreta, causing environmental pollution [2,3]. Tetracycline, as the second class of antibiotics, has been widely used in agriculture and animal husbandry [4]. At present, tetracycline has been detected in many rivers and lakes. Therefore, how to remove the residual tetracycline from environment has become a hot topic of current research [5].

So far, many methods have been used to remove tetracycline in water, such as adsorption [6–8], membrane separation [9,10], photocatalytic method [11,12] and activated sludge [13], etc. The adsorption method is preferred because of its low cost, high efficiency, simplicity and environmental protection [14]. In recent years, it has been found that multi-component composite metal oxides have unique properties and advantages such as strong selectivity, large specific surface area, high adsorption capacity, and can complement each other. Therefore, more and more researchers have devoted themselves to the study of multi-component metal oxides.

\* Corresponding author.

In the relevant literatures, iron and manganese oxides have good adsorption properties for pollutants in the environment due to their many active functional groups of iron elements, good pore structure [15] and synergistic effect between components. Manganese oxide is considered to be an effective low-temperature catalyst to modify the adsorbent to enhance the mineralization of adsorbed tetracycline (TC). In addition, iron has a high element abundance in the first transition system, which is not only low in cost, but also has a certain affinity for TC.

In this study, Fe, Mn and Ce were composited into metal oxides by using a simple co-precipitation method. The microstructure and elemental composition of the adsorbents were systematically studied. Meantime, the adsorption behavior of TC onto Fe-Mn-Ce metal oxides (FeMC) and cyclic stability of FeMC were also evaluated under different conditions. In addition, the interface mechanism between FeMC and TC was discussed.

## 2. Experimental part

### 2.1. Reagents and instruments

The iron trichloride hexahydrate ( $\text{FeCl}_3 \cdot 6\text{H}_2\text{O}$ ), cerium nitrate hexahydrate ( $\text{Ce}(\text{NO}_3)_3 \cdot 6\text{H}_2\text{O}$ ), hydrochloric acid (HCl), sodium hydroxide (NaOH) were purchased from Sinopharm Chemical Reagent Co., Ltd., (Ningbo Road, Shanghai); manganese acetate tetrahydrate ( $\text{Mn}(\text{CH}_3\text{COO})_2 \cdot 4\text{H}_2\text{O}$ ) was purchased from Tianjin Institute of Fine Chemicals (Nankai University Farm, Nankai District, Tianjin); ammonia ( $\text{NH}_3 \cdot \text{H}_2\text{O}$ ) and anhydrous ethanol were purchased from Xilong Technology Co., Ltd., (China). Deionized water was prepared by FST-TOP-A24 UltraPure water mechanism of Shanghai Foster Instrument Co., Ltd., (Gucheng Road, Jinshan District, Shanghai, China). TC solutions were prepared with deionized water. The pH of the TC solution was tested by the PHS-3C pH Meter (Shanghai Yidian Scientific Instrument Co., Ltd., Yuanda Road, Anting Town, Jiading District, Shanghai, China). Ultraviolet spectrophotometer (UV-2600i) came from Shimadzu, Japan. Air Blast Drying Box (DHG-9023), muffle furnace (9XL-1008) and Teflon lined stainless steel autoclave were used to synthesize composites.

### 2.2. Preparation of adsorbent

FeMC composite metal oxides were prepared by coprecipitation method. The specific preparation process is as follows: a certain amount of  $\text{FeCl}_3 \cdot 6\text{H}_2\text{O}$ ,  $\text{Mn}(\text{CH}_3\text{COO})_2 \cdot 4\text{H}_2\text{O}$  and  $\text{Ce}(\text{NO}_3)_3 \cdot 6\text{H}_2\text{O}$  solid were dissolved in 60 mL deionized water. Then add a certain amount of ammonia as precipitant, and adjust the solution pH to 9. The precipitate was strongly stirred for 2 h with a magnetic stirrer. After aging for 4 h, the precipitate was filtered and separated. The obtained precipitate was washed several times with deionized water, then dried in an oven at 105°C for 12 h, and calcined at 400°C for 3 h to obtain the final experimental materials.

### 2.3. Characterizations of samples

The surface morphology and structure of FeMC nano-composite was characterized by field-emission scanning

electron microscopy (FE-SEM, AURIGA, ZEISS Company, Germany) coupled with an energy-dispersive X-ray spectrometer (EDS, INCA X-Max 50, ZEISS Company, Germany). The X-ray diffractometer (XRD, PANalytical, The Netherlands) with a Cu K $\alpha$  source was used to analyze the crystalline structure. Fourier-transform infrared spectroscopy (FT-IR, Nexus-870, Thermo Nicolet, USA) was used to determine the change of surface properties. The nano zeta potential analyzer (ZETA, Zetasizer Nano, Malvern Instruments, UK) was used to analyze the zeta potential of the adsorbent before and after adsorption.

### 2.4. Batch adsorption experiment

#### 2.4.1. Effect of adsorption kinetics

The 25 mg adsorbent was added into 100 mL TC solution (20 mg/L). Then, the adsorption kinetics was studied at 25°C. In the experiment, the adsorbent was added to 100 mL TC solution (20 mg/L), then oscillated in a constant temperature oscillator at 25°C and 160 rpm. 3 mL suspension was taken at different times and filtered by 0.22  $\mu\text{m}$  inorganic filter membrane. The absorbance at 350 nm was measured by ultraviolet spectrophotometer.

#### 2.4.2. Effect of initial pH of TC solution on adsorption performance

In 100 mL TC solution (20 mg/L), the pH value of TC solution was adjusted to 3–12 by 0.1 mol/L HCl and 1 mol/L NaOH solution, and the pH value was detected by PHB-3 digital pH meter. Then, 25 mg of adsorbent was added, and the constant temperature oscillator was shaded at 25°C and 160 rpm for 12 h. Finally, 3 mL suspension was extracted, filtered with 0.22  $\mu\text{m}$  inorganic filter membrane and measured by ultraviolet spectrophotometer.

#### 2.4.3. Adsorption isotherms

In the isothermal adsorption experiment, 25 mg adsorbent was added to 100 mL TC solution with different concentrations (20–100 mg/L), and shake at 25°C, 160 rpm in constant temperature oscillator. During the oscillation period, 3 mL supernatant was extracted at different time points and filtered with 0.22  $\mu\text{m}$  inorganic filter membrane. The absorbance was measured by ultraviolet spectrophotometer, and the adsorption isotherms were tested at three temperatures (25°C, 35°C, and 45°C).

#### 2.4.4. Cyclic regeneration

Firstly, TC adsorbed on FeMC composite metal oxides was desorbed with 0.1 mol/L NaOH for 5 h [16]. Then, the adsorbent was washed with deionized water until pH was neutral and dried in an oven at 40°C for 8 h. Then the sample was put into 100 mL TC solution (20 mg/L), and under the condition of 25°C, 160 rpm shading oscillation 12 h. The suspension was extracted 3 mL, filtered with 0.22  $\mu\text{m}$  inorganic filter membrane and measured by ultraviolet spectrophotometer. Finally, under the same experimental conditions, four cycles of regeneration experiments were repeated according to the above steps.

### 2.5. Analysis and data processing

The removal efficiency of TC and the saturated adsorption capacity of the adsorbent were calculated by Eqs. (1) and (2):

$$n(\%) = \frac{C_0 - C_e}{C_0} \times 100\% \quad (1)$$

$$q_e = \frac{(C_0 - C_e)V}{W} \quad (2)$$

where  $n$  (%) is the removal efficiency of TC;  $q_e$  (mg/g) is the adsorption capacity of adsorbents in the adsorption equilibrium point;  $C_0$ ,  $C_e$  (mg/L) are the initial and equilibrium TC concentrations of the solution, respectively.  $V$  (L) is the volume of TC solution;  $W$  (g) is the dosage of adsorbents.

Adsorption kinetics experimental data processing using pseudo-first-order kinetics and pseudo-second-order kinetics, equation expression is as Eqs. (3) and (4):

$$\log(q_e - q_t) = \log q_e - \frac{k_1 t}{2.303} \quad (3)$$

$$\frac{t}{q_t} = \frac{1}{k_2 q_e^2} + \frac{t}{q_e} \quad (4)$$

where  $q_e$  (mg/g) is the adsorption amount of TC at equilibrium time;  $q_t$  (mg/g) is the adsorption amount of TC at time  $t$ , and  $t$  (min) is the adsorption time;  $k_1$  ( $\text{min}^{-1}$ ) and  $k_2$  ( $\text{g}/(\text{mg}\cdot\text{min})$ ) are the rate constants of pseudo-first-order kinetics and pseudo-second-order kinetics, respectively.

The intraparticle diffusion model is based on diffusion and is used to describe competitive adsorption and multi-stage adsorption, including the transfer of adsorbed molecules from the aqueous phase to the adsorbent surface, penetration into the internal space of the adsorbent [17]. The kinetic equation of intraparticle diffusion is expressed as Eq. (5):

$$q_t = k_p t^{1/2} + I \quad (5)$$

where  $q_t$  (mg/g) and  $k_p$  ( $\text{mg}/\text{g}\cdot\text{min}^{0.5}$ ) pollutant capacity adsorbed at equilibrium the constant rate of adsorption is the intraparticle diffusion model, respectively.

Langmuir and Freundlich adsorption models were used for data processing of adsorption isotherms. The Langmuir isotherm was used to describe monolayer adsorption, in which adsorption occurred on a specific uniform surface containing sites with equal energy. The Freundlich isotherm was used to describe multilayer adsorption with interactions and the adsorption process occurring at specific heterogeneous surface energies [18]. The equation expression was presented as Eqs. (6) and (7):

$$\frac{C_e}{q_e} = \frac{C_e}{q_m} + \frac{1}{K_L \times q_m} \quad (6)$$

$$\ln q_e = \frac{1}{n} \ln C_e + \ln K_F \quad (7)$$

where  $C_e$  (mg/L) is the TC concentration after equilibrium adsorption;  $q_e$  (mg/g) is the TC content of the equilibrium adsorbent;  $q_m$  (mg/g) is the maximum adsorption capacity calculated according to the Langmuir equation;  $K_L$  is Langmuir adsorption constant,  $K_F$  and  $n$  are Freundlich adsorption constant.

The experimental data of adsorption thermodynamics were processed by Gibbs equation, and the equations were expressed as Eqs. (8)–(10):

$$\Delta G = \Delta H - T\Delta S \quad (8)$$

$$\Delta G = -RT \ln K \quad (9)$$

$$\ln K = \frac{\Delta S}{R} - \frac{\Delta H}{RT} \quad (10)$$

where  $\Delta H$  is enthalpy change;  $\Delta G$  is Gibbs free energy and  $\Delta S$  is entropy change;  $R$  stands for the gas constant ( $R = 8.314 \text{ J}/\text{mol}\cdot\text{K}$ ), and  $T$  stands for the absolute temperature (K).  $K$  is the adsorption equilibrium constant ( $q/C_e$ ).

## 3. Results and discussion

### 3.1. SEM analysis

As can be seen from Fig. 1a and b, the prepared samples are composed of irregular nanoparticles with a particle size of about 50–100 nm. The surface of the samples is rough and uneven, and the pore or gap structure is generated by the accumulation of many nanoparticles. Fig. 1c and d is the morphology of the FeMC sample after adsorption. It is obvious that the pores between the particles are filled with a large amount of TC, and the surface of the sample is also attached to TC, which fully shows that the adsorption performance of the FeMC sample is better.

### 3.2. EDS analysis

EDS spectrum can be used to further analyze the elemental composition of FeMC adsorbent. The elemental content and elemental analysis spectrum are shown in Table 1 and Fig. 2. It can be seen from the elemental spectrum and content table that C, O, Mn, Fe and Ce are the basic elements that constitute the FeMC adsorbent. Combined with Fig. 1a and b, it indicates that the FeMC adsorbent has been synthesized successfully.

### 3.3. XRD analysis

The structural characteristics of FeMC adsorbent were studied by XRD, and the results are shown in Fig. 3. For the prepared FeMC adsorbent, no visible characteristic peaks of Mn species were observed, and the existence of Mn element was found by EDS spectrum, which may be that Mn species are highly dispersed on the surface of the adsorbent or exist in amorphous state. At the same time, the peaks of the adsorbent at  $2\theta$  of  $28.55^\circ$ ,  $47.49^\circ$ ,  $56.34^\circ$ ,  $69.40^\circ$  and  $79.07^\circ$  are attributed to the (111), (220), (311), (400) and (420) diffraction peaks of  $\text{CeO}_2$  (PDF # 34-0394). In addition, the characteristic diffraction peak of  $\text{Fe}_2\text{O}_3$  (PDF # 33-0664) appeared at  $2\theta = 33.08^\circ$ .

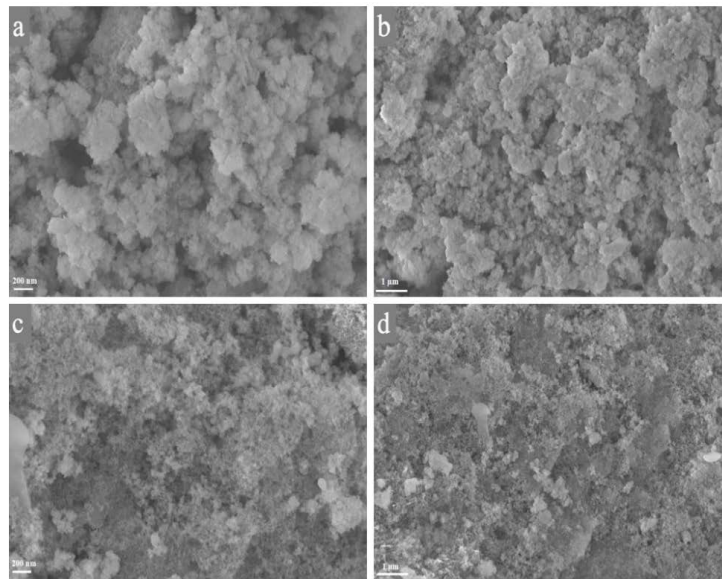


Fig. 1. (a,b) Scanning electron microscopy images before adsorption of FeMC adsorbent and (c,d) scanning electron microscopy images after adsorption of tetracycline solution by FeMC adsorbent.

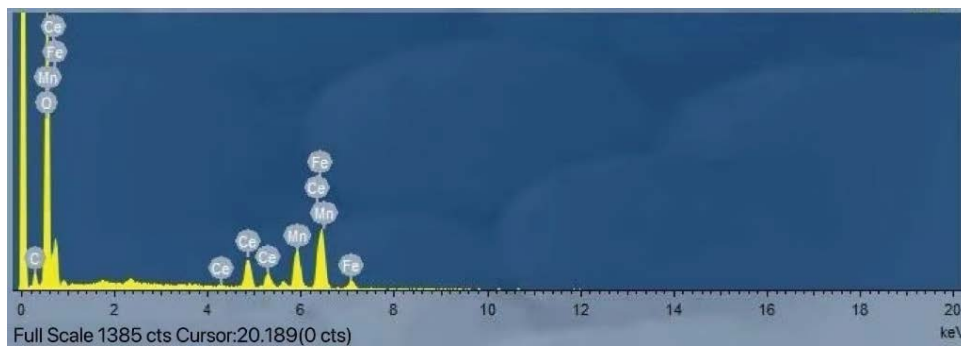


Fig. 2. Energy-dispersive X-ray spectrum of FeMC adsorbent.

Table 1  
Element content of FeMC adsorbent

Element	Atomic (%)
C K	10.36
O K	58.63
Mn K	9.15
Fe K	17.23
Ce L	4.63
Total	100

### 3.4. Adsorption performance

#### 3.4.1. Adsorption isotherm

The relationship between adsorbate equilibrium concentration and adsorption capacity can be reflected by the adsorption isotherms [19]. Langmuir model is based on the following aspects: (1) the adsorbent surface is uniform; (2) the energy of each adsorption center is equivalent; (3) and the

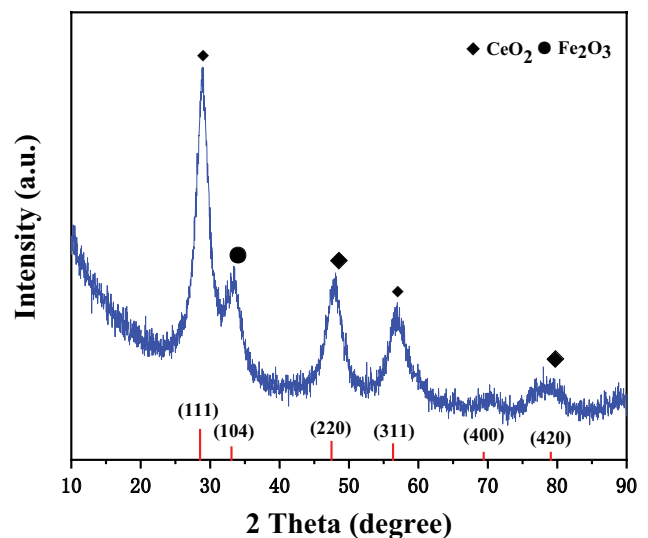


Fig. 3. X-ray diffraction patterns of FeMC adsorbent.

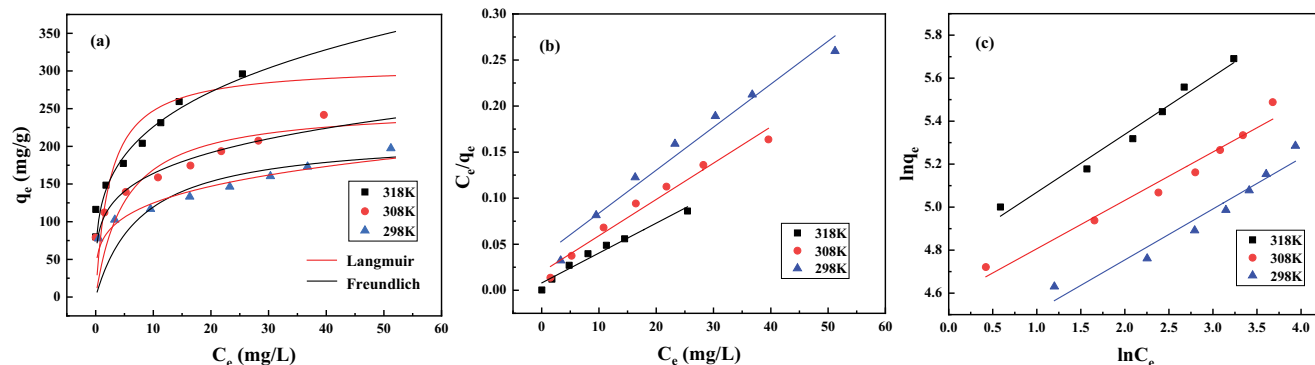


Fig. 4. (a) Isotherm of tetracycline adsorption by FeMC and (b,c) are linear fitting curves of Langmuir and Freundlich models, respectively. ( $C_0 = 20\text{--}100\text{ mg/L}$ , adsorbent dose =  $0.25\text{ g/L}$ ).

interaction force between adsorbed molecules is negligible. By contrast, Freundlich model is based on the heterogeneity of solid surface [20]. The adsorption isotherm of TC on FeMC is shown in Fig. 4, and the fitting isotherm parameters are summarized in Table 2. By comparing the  $R^2$  values of Langmuir model and Freundlich model, Langmuir model has a higher correlation coefficient than the Freundlich model, which can better describe the adsorption process, indicating that TC is uniformly adsorbed on FeMC adsorbent, and monolayer adsorption is the main interaction mechanism [21]. In addition, the Langmuir isotherm model showed that the maximum adsorption capacities of TC at 298, 308 and 318 K were 214.133, 253.807 and 307.692 mg/g, respectively, indicating that increasing temperature was conducive to adsorption. The constant  $K_F$  obtained from Freundlich isotherm model is an indicator of adsorption capacity, and  $n$  is a constant indication of the degree of heterogeneity and indicates how favorable the adsorption process is. When the value of  $1/n$  is less than 1, the adsorption reaction is a favorable adsorption process and spontaneous [22]. The  $K_F$  values at different temperatures were  $298 < 308 < 318\text{ K}$ , which was consistent with the results obtained from the Langmuir isotherm model, and the  $n$  values at all temperatures were between 1 and 10, indicating that the adsorbent had a good absorption effect. These results are consistent with the kinetic fitting results, indicating that the adsorption mechanism involves chemical adsorption process.

### 3.4.2. Adsorption kinetics

The adsorption kinetics can be used to describe the adsorption rate and suitable contact time on TC removal in adsorbents [23]. In order to further study the adsorption mechanism and control steps of FeMC on TC, the pseudo-first-order and pseudo-second-order kinetic models were used to fit and analyze the experimental data. Pseudo-first-order model describes the process in which pollutants are adsorbed to the surface by overcoming surface resistance through physical diffusion and physical interaction [24]. Pseudo-second-order model indicates that chemical interaction is the main factor for controlling the adsorption rate, and the adsorption process dominated by chemical adsorption generally has the highest fitting degree [25].

Table 2

Fitting parameters of isotherm model for tetracycline adsorption by FeMC

Model	Langmuir			Freundlich		
	$T$ (K)	$K_L$	$q_m$	$R^2$	$n$	$K_F$
298	0.126	214.133	0.965	4.220	72.292	0.935
308	0.199	253.807	0.965	4.441	97.628	0.959
318	0.409	307.692	0.970	3.710	121.467	0.969

The fitting results are shown in Fig. 5 and Table 3. As shown in Fig. 5a, the adsorption amount of TC increased rapidly in the first 400 min, and the adsorption amount gradually decreased with the decrease of the number of active sites of FeMC adsorbent. The adsorption process gradually reached equilibrium after 720 min. According to the kinetic fitting parameter table, compared with the correlation coefficient fitted by the pseudo-first-order kinetic model ( $R^2 = 0.992$ ), the correlation coefficient fitted by the pseudo-second-order kinetic model ( $R^2 = 0.994$ ) is high relatively. It indicates that the pseudo-second-order kinetic model can more accurately describe the adsorption process of FeMC on TC [26].

In addition, the adsorption process is presented in Fig. 5d, which has been divided into two stages: first, the contaminant diffuses around the adsorbent; then it overcomes the resistance of the liquid and diffuses to the surface of the adsorbent; and the second phase diffuses from the outer surface to the inner surface. Since the initial diffusion process and binding to the adsorption site are independent, membrane diffusion and internal diffusion are the main factors for controlling the adsorption [27]. As shown in Fig. 5d, the large slope of the first stage should correspond to the membrane diffusion, when TC rapidly diffuses to the surface of FeMC adsorbent. In the second phase, the adsorption rate gradually slows down, and internal diffusion begins to replace membrane diffusion as the main control mechanism of the adsorption process, and a large number of TC molecules may diffuse into the spatial structure of the FeMC adsorbent. The adsorption rate is controlled by both internal diffusion and membrane diffusion since the cut-off in both phases does not pass through the origin [28].

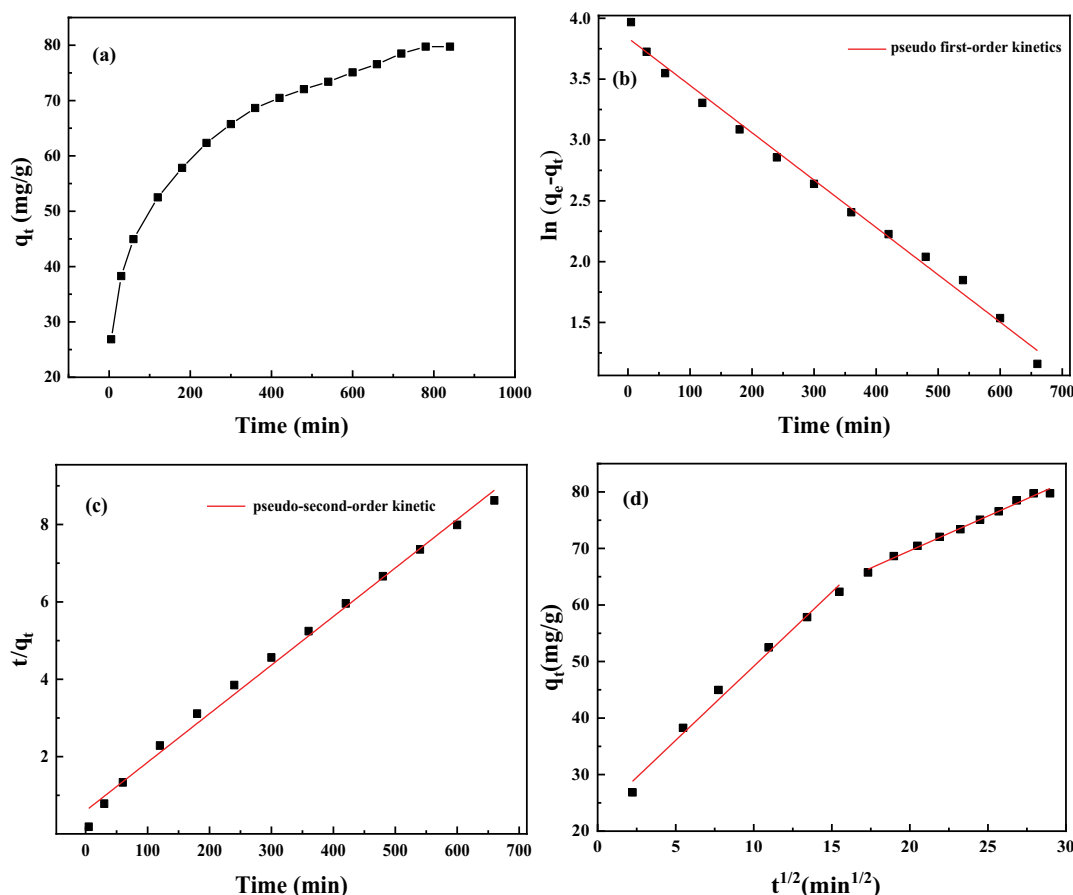


Fig. 5. (a) Kinetic experimental data of tetracycline adsorption by FeMC, (b) pseudo-first-order kinetic curve, and (c) pseudo-second-order kinetic curve, and (d) intraparticle diffusion model. ( $C_0 = 20 \text{ mg/L}$ , adsorbent dose =  $0.25 \text{ g/L}$ ,  $T = 298 \text{ K}$ ).

Table 3  
Quasi-first-order and second-order kinetic fitting parameters of tetracycline adsorption by FeMC

Pseudo-first-order kinetics			Pseudo-second-order kinetics		
$k_1 \text{ (min}^{-1}\text{)}$	$q_e \text{ (mg/g)}$	$R^2$	$k_2 \text{ (g/(mg}\cdot\text{min))}$	$q_e \text{ (mg/g)}$	$R^2$
0.009	46.435	0.992	$0.263 \times 10^{-3}$	79.618	0.994

Table 4  
Thermodynamic parameters of tetracycline adsorption by FeMC

Parameters	$T \text{ (K)}$	$\Delta G \text{ (kJ/mol)}$	$\Delta S \text{ (kJ/K}\cdot\text{mol)}$	$\Delta H \text{ (kJ/mol)}$
	298	-3.341		
FeMC	308	-4.634	0.129	35.178
	318	-6.487		

### 3.4.3. Adsorption thermodynamics

Adsorption thermodynamics can reveal the variation law of adsorption process with the change of temperature [26]. Through the study of adsorption thermodynamics, the transfer and change of heat energy during the adsorption of TC by FeMC at different temperatures were analyzed. Table 4 shows that  $\Delta H$  value is greater than zero, indicating that TC adsorption is an endothermic process. In addition, the  $\Delta H$  value was  $35.178 \text{ kJ/mol}$ , indicating that chemical adsorption was dominant, accompanied by physical adsorption [29]. With the increase of adsorption temperature from 298 to 318 K, the  $\Delta G$  value decreased slightly, indicating that the increase of temperature enhanced the adsorption force. The  $\Delta G$  value was less than zero, so the adsorption process was spontaneous [30].

### 3.4.4. Effect of initial pH

The influence of the zeta potential of the adsorbent and the pH of the aqueous solution on TC adsorption and the exploration of the adsorption mechanism are important. The zeta potential was measured under neutral conditions to study the surface charge of the FeMC adsorbent in aqueous solution [31]. The pH value where the zeta potential was zero was taken as the isoelectric point (IEP). It can be seen from Fig. 6 that when the pH increased from 3 to 12, the zeta potential gradually decreased from  $12.76$  to  $-21.8 \text{ mV}$ , and the point of zero charge (PZC) of FeMC is 9.12.

The previous study showed that TC was an amphoteric molecule [32] and solution pH was also a significant factor to affect the surface charge of adsorbent. In this study, the influence of pH on the TC removal was investigated in the

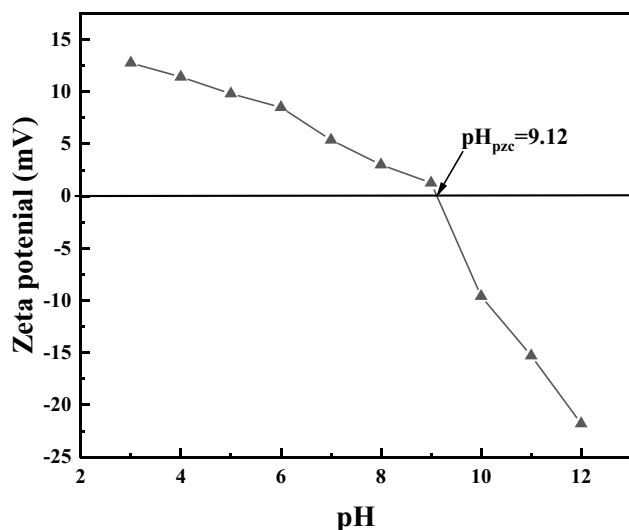


Fig. 6. Zeta potential of FeMC adsorbent.

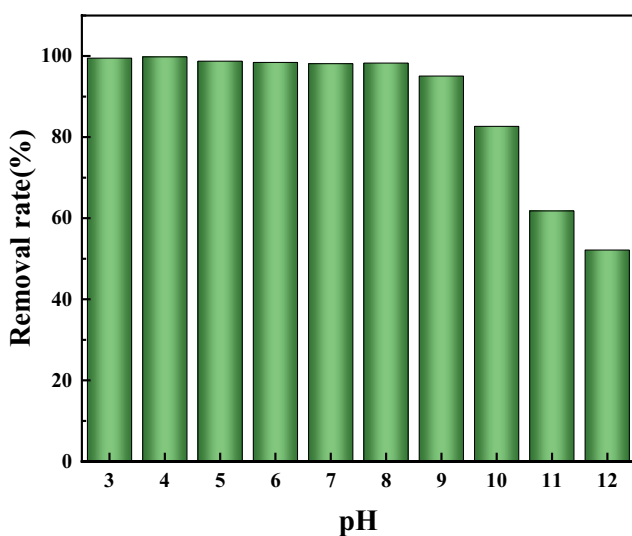


Fig. 7. Effect of pH on tetracycline removal by FeMC adsorbent. ( $C_0 = 20$  mg/L, adsorbent dose = 0.25 g/L,  $T = 298$  K).

pH range 3–12. The effect of pH value on the removal efficiency of TC is shown in Fig. 7. When the pH value of TC solution increases from 3 to 12, the removal rate of TC by FeMC decreases and reaches 99.81% at pH 4. According to the study conducted by Jin [33], the TC is positively charged forms when  $\text{pH} < 3.3$ , neutral forms as pH ranges from 3.3 to 7.7, and negatively charged forms when the  $\text{pH} > 7.7$ . When pH is 3, some metal oxides in FeMC adsorbent may dissolve, so the removal rate of TC decreases slightly. When the pH value is in the range of 4–9, TC molecules mainly become amphoteric ions and anions, and the surface charge of FeMC maintains positive charge, resulting in electrostatic attraction. However, when  $\text{pH} \geq 9$ , the removal rate of TC decreased significantly due to the increased electrostatic repulsion between TC and negatively charged FeMC ( $\text{pH}_{\text{pzc}} = 9.12$ ).

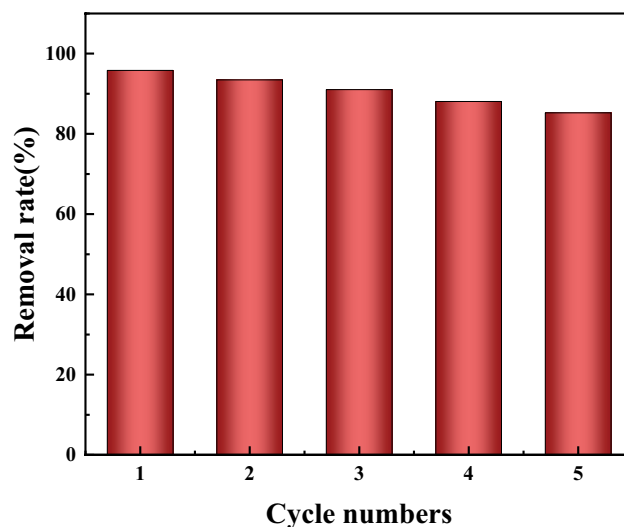


Fig. 8. Reusability of Fe-Mn-Ce for tetracycline adsorption experiments. ( $C_0 = 20$  mg/L, adsorbent dose = 0.25 g/L,  $T = 298$  K).

#### 3.4.5. Reusability of Fe-Mn-Ce for TC adsorption

The practical application of adsorbent is closely related to its regeneration performance. Here the regeneration of adsorbent was studied as an important parameter to evaluate its stability. As shown in Fig. 8, after five cycles, the removal rate decreased slightly, which was mainly due to the loss of loaded iron and the irreversibility of some adsorption sites [34]. However, after five cycles, the removal rate of TC still reached 85.24%, indicating that FeMC is an ideal adsorbent for the removal of TC in water.

#### 3.5. Comparison with other adsorbents

The adsorption properties of different adsorbents for TC were compared in Table 5. It can be seen from Table 5 that the maximum adsorption capacity ( $Q_m$ ) of FeMC for TC at the same temperature is higher than other adsorbents. The results show that FeMC is an ideal material for removing TC.

#### 3.6. Adsorption mechanism

The functional group of the adsorbent is one of the important factors affecting the adsorption efficiency. As shown in Fig. 9, FT-IR was applied to analyze the TC on FeMC before and after TC adsorption to further elucidate the mechanism. According to previous studies, the peak at  $3,395\text{ cm}^{-1}$  were ascribed to O–H stretching vibrations, implying the existence of carboxylic, hydroxyl and chemisorbed water [42]. The peak at  $1,616\text{ cm}^{-1}$  were assigned to C=C or C=O stretching vibrations [42,43]. While the peak at  $1,111\text{ cm}^{-1}$  is caused by the bending vibration of structural –OH [44]. After reacting with TC, new characteristic peaks appeared at  $1,453$  and  $1,045\text{ cm}^{-1}$ , where the peak at  $1,453\text{ cm}^{-1}$  corresponds to the aliphatic C–H stretching vibration of TC [45] and the peak at  $1,045\text{ cm}^{-1}$  is attributed to the C–O or C–O–C stretching vibration of TC [46,47]. This indicates that TC was successfully adsorbed on FeMC, and the adsorption

Table 5  
Comparison of the  $Q_m$  of tetracycline with various types of adsorbents

Adsorbents	Tetracycline concentration (mg/L)	$T$ ( $^{\circ}\text{C}$ )	$Q_m$ (mg/g)	References
$\text{Fe}_3\text{O}_4$ nanoparticles	10	25	40.07	[22]
Cu-bent	20	25	39.29	[35]
MAIlg-Fe-Cu	20	25	130.72	[36]
CA-CNTs	30	25	195.90	[37]
La-modified magnetic composite	25	25	146.00	[38]
Zn-LBC	10	30	159.64	[39]
Fe/Zn-SBC	30	25	145.00	[40]
$\text{AgO/MgO/FeO/Si}_3\text{N}_4$	30	30	172.41	[41]
Fe-Mn-Ce	20	25	214.13	This study
	20	35	253.81	

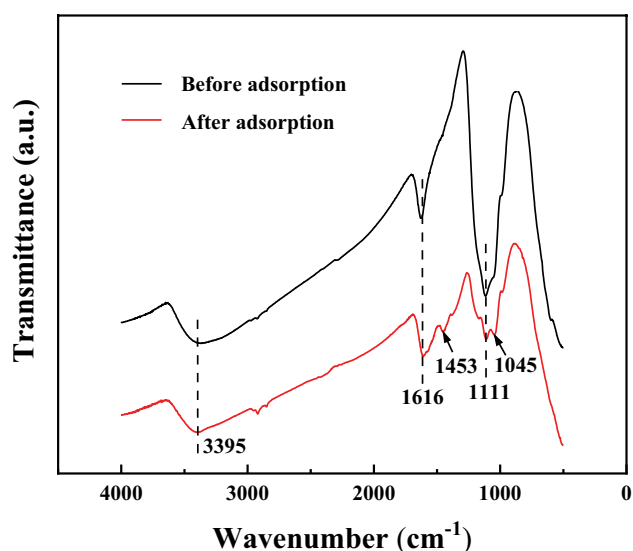


Fig. 9. Fourier-transform infrared spectroscopy images of FeMnCe adsorbent.

between them was achieved through electron sharing and the formation of chemical bonds between functional groups.

From discussion mentioned above based on isotherm and kinetic studies, the adsorption of tetracycline on FeMC was mainly controlled by chemisorption. The adsorption is consistent with the Langmuir model and the proposed secondary kinetics and is dominated by chemisorption [48–50]. Also, the  $\Delta H$  and  $\Delta G$  values in the thermodynamic studies indicate the presence of chemisorption and that this chemisorption is heat absorbing and spontaneous [51,52]. According to the properties of PZC and TC of FeMC, there is electrostatic repulsion between FeMC and TC at  $\text{pH} = 3$ . When  $\text{pH} = 4$ – $9$ , there is electrostatic attraction effect; when  $\text{pH} > 9$ , there is electrostatic repulsion effect. Therefore, the electrostatic interactions between positively charged FeMC and amphipathic ions TC are important for adsorption. The results suggest that TC was successfully adsorbed onto FeMC, while electrostatic adsorption plays a significant role during the adsorption process.

#### 4. Conclusions

In summary, Fe-Mn-Ce composite metal oxides were synthesized by co-precipitation method, and were systematically characterized and used to adsorb tetracycline in water. The experimental results show that FeMC adsorbent has a wide pH range, and the removal rate of TC is more than 90% at pH 3–9. The FeMC has a good TC removal performance, and its maximum adsorption capacity is up to 307.692 mg/g. The reusability study showed that the adsorption performance of FeMC still reached 85.24% after five cycles. At the same time, the removal process of TC by FeMC adsorbent conforms to the pseudo-second-order kinetic model and Langmuir model, indicating that chemical adsorption and monolayer adsorption are the main interaction mechanisms. In addition, the Gibbs free energy indicates that the removal of TC by FeMC adsorbent is a spontaneous endothermic process. In this study, a simple, efficient and reusable adsorbent (Fe/Mn/Ce composite metal oxides) for TC removal was developed.

#### Acknowledgments

The authors are especially grateful to the Project of 2022 Provincial Quality Engineering Project for Higher Education Institutions of Anhui Province (2022jyxm276), the Natural Science Research Project of the Higher Education Institutions of Anhui Province (KJ2021A0616, KJ2020A0468), the Scientific Research Start-up Foundation for Introduction of Talent, Anhui Jianzhu University (2020QDZ28, 2016QD113), the National Natural Science Foundation of China (61873003), the Natural Science Foundation of Anhui Province (1908085QE241) and the first batch of natural science projects supported by surplus funds in 2021 of Anhui Jianzhu University (JZ202129, JZ202134).

#### References

- [1] J. Liu, H. Lin, Y. Dong, Y. He, W. Liu, Y. Shi, The effective adsorption of tetracycline onto  $\text{MoS}_2/\text{Zeolite-5}$ : adsorption behavior and interfacial mechanism, *J. Environ. Chem. Eng.*, 9 (2021) 105912, doi: 10.1016/j.jece.2021.105912.
- [2] W. Xu, G. Zhang, X. Li, S. Zou, P. Li, Z. Hu, J. Li, Occurrence and elimination of antibiotics at four sewage treatment plants

- in the Pearl River Delta (PRD), South China, *Water Res.*, 41 (2007) 4526–4534.
- [3] B. Hong, Q. Lin, S. Yu, Y. Chen, Y. Chen, P. Chiang, Urbanization gradient of selected pharmaceuticals in surface water at a watershed scale, *Sci. Total Environ.*, 634 (2018) 448–458.
- [4] X. Zhang, Y. Li, M. Wu, Y. Pang, Z. Hao, M. Hu, R. Qiu, Z. Chen, Enhanced adsorption of tetracycline by an iron and manganese oxides loaded biochar: kinetics, mechanism and column adsorption, *Bioresour. Technol.*, 320 (2021) 124264, doi: 10.1016/j.biortech.2020.124264.
- [5] J. Pan, X. Bai, Y. Li, B. Yang, P. Yang, F. Yu, J. Ma, HKUST-1 derived carbon adsorbents for tetracycline removal with excellent adsorption performance, *Environ. Res.*, 205 (2022) 112425, doi: 10.1016/j.envres.2021.112425.
- [6] Y. Yue, C. Shen, Y. Ge, Biochar accelerates the removal of tetracyclines and their intermediates by altering soil properties, *J. Hazard. Mater.*, 380 (2019) 120821, doi: 10.1016/j.jhazmat.2019.120821.
- [7] J.O. Eniola, R. Kumar, A.A. Al-Rashdi, M.A. Barakat, Hydrothermal synthesis of structurally variable binary CuAl, MnAl and ternary CuMnAl hydroxides for oxytetracycline antibiotic adsorption, *J. Environ. Chem. Eng.*, 8 (2020) 103535, doi: 10.1016/j.jece.2019.103535.
- [8] N. Saman, N.S. Othman, L.-Y. Chew, Cetyltrimethylammonium bromide functionalized silica nanoparticles (MSN) synthesis using a combined sol-gel and adsorption steps with enhanced adsorption performance of oxytetracycline in aqueous solution, *J. Taiwan Inst. Chem. Eng.*, 112 (2020) 67–77.
- [9] B.L. Phoon, C.C. Ong, M.S. Mohamed Saheed, P.-L. Show, J.-S. Chang, T.C. Ling, S.S. Lam, J.C. Juan, Conventional and emerging technologies for removal of antibiotics from wastewater, *J. Hazard. Mater.*, 400 (2020) 122961, doi: 10.1016/j.jhazmat.2020.122961.
- [10] T. Lu, X. Xu, X. Liu, T. Sun, Super hydrophilic PVDF based composite membrane for efficient separation of tetracycline, *Chem. Eng. J.*, 308 (2017) 151–159.
- [11] M. Minale, Z. Gu, A. Guadie, D.M. Kabtamu, Y. Li, X. Wang, Application of graphene-based materials for removal of tetracyclines using adsorption and photocatalytic-degradation: a review, *J. Environ. Manage.*, 276 (2020) 111310, doi: 10.1016/j.jenvman.2020.111310.
- [12] A. Majumdar, U. Ghosh, A. Pal, Novel 2D/2D g-C<sub>3</sub>N<sub>4</sub>/Bi<sub>4</sub>NbO<sub>8</sub>Cl nano-composite for enhanced photocatalytic degradation of oxytetracycline under visible LED light irradiation, *J. Colloid Interface Sci.*, 584 (2021) 320–331.
- [13] Q. Xu, B. Han, H. Wang, Q. Wang, W. Zhang, D. Wang, Effect of extracellular polymer substances on the tetracycline removal during coagulation process, *Bioresour. Technol.*, 309 (2020) 123316, doi: 10.1016/j.biortech.2020.123316.
- [14] H. Mazaheri, M. Ghaedi, M.H. Ahmadi Azghandi, A. Asfaram, Application of machine/statistical learning, artificial intelligence and statistical experimental design for the modeling and optimization of methylene blue and Cd(II) removal from a binary aqueous solution by natural walnut carbon, *Phys. Chem. Chem. Phys.*, 19 (2017) 11299–11317.
- [15] J. Liang, Y. Fang, Y. Luo, G. Zeng, J. Deng, X. Tan, N. Tang, X. Li, X. He, C. Feng, S. Ye, Magnetic nanoferrromanganese oxides modified biochar derived from pine sawdust for adsorption of tetracycline hydrochloride, *Environ. Sci. Pollut. Res.*, 26 (2019) 5892–5903.
- [16] Y.-K. Choi, T.-R. Choi, R. Gurav, S.K. Bhatia, Y.-L. Park, H.J. Kim, E. Kan, Y.-H. Yang, Adsorption behavior of tetracycline onto *Spirulina* sp. (microalgae)-derived biochars produced at different temperatures, *Sci. Total Environ.*, 710 (2020) 136282, doi: 10.1016/j.scitotenv.2019.136282.
- [17] S.A.R. Ahmadi, M.R. Kalae, O. Moradi, F. Nosratinia, M. Abdouss, Synthesis of novel zeolitic imidazolate framework (ZIF-67)-zinc oxide (ZnO) nanocomposite (ZnO@ZIF-67) and potential adsorption of pharmaceutical (tetracycline (TCC)) from water, *J. Mol. Struct.*, 1251 (2022) 132013, doi: 10.1016/j.molstruc.2021.132013.
- [18] Y. Bao, Q. Zhou, Y. Wan, Q. Yu, X. Xie, Effects of soil/solution ratios and cation types on adsorption and desorption of tetracycline in soils, *Soil Sci. Soc. Am. J.*, 74 (2010) 1553–1561.
- [19] H. Qiao, X. Wang, P. Liao, C. Zhang, C. Liu, Enhanced sequestration of tetracycline by Mn(II) encapsulated mesoporous silica nanoparticles: synergistic sorption and mechanism, *Chemosphere*, 284 (2021) 131334, doi: 10.1016/j.chemosphere.2021.131334.
- [20] L. Yan, Y. Liu, Y. Zhang, S. Liu, C. Wang, W. Chen, C. Liu, Z. Chen, Y. Zhang, ZnCl<sub>2</sub> modified biochar derived from aerobic granular sludge for developed microporosity and enhanced adsorption to tetracycline, *Bioresour. Technol.*, 297 (2020) 122381, doi: 10.1016/j.biortech.2019.122381.
- [21] Y. Gao, Y. Li, L. Zhang, H. Huang, J. Hu, S.M. Shah, X. Su, Adsorption and removal of tetracycline antibiotics from aqueous solution by graphene oxide, *J. Colloid Interface Sci.*, 368 (2012) 540–546.
- [22] W. Zhai, J. He, P. Han, M. Zeng, X. Gao, Q. He, Adsorption mechanism for tetracycline onto magnetic Fe<sub>3</sub>O<sub>4</sub> nanoparticles: adsorption isotherm and dynamic behavior, location of adsorption sites and interaction bonds, *Vacuum*, 195 (2022) 110634, doi: 10.1016/j.vacuum.2021.110634.
- [23] B. Debnath, M. Majumdar, M. Bhowmik, K.L. Bhowmik, A. Debnath, D.N. Roy, The effective adsorption of tetracycline onto zirconia nanoparticles synthesized by novel microbial green technology, *J. Environ. Manage.*, 261 (2020) 110235, doi: 10.1016/j.jenvman.2020.110235.
- [24] B. Chen, Y. Li, Q. Du, X. Pi, Y. Wang, Y. Sun, M. Wang, Y. Zhang, K. Chen, J. Zhu, Effective removal of tetracycline from water using copper alginate @ graphene oxide with in-situ grown MOF-525 composite: synthesis, characterization and adsorption mechanisms, *Nanomaterials*, 12 (2022) 2897, doi: 10.3390/nano12172897.
- [25] Y. Zhang, Z. Huang, X. Fang, Y. Chen, S. Fan, H. Xu, Preparation of magnetic porous biochar through hydrothermal pretreatment combined with K<sub>2</sub>FeO<sub>4</sub> activation to improve tetracycline removal, *Microporous Mesoporous Mater.*, 343 (2022) 112188, doi: 10.1016/j.micromeso.2022.112188.
- [26] F. Jia, D. Zhao, M. Shu, F. Sun, D. Wang, C. Chen, Y. Deng, X. Zhu, Co-doped Fe-MIL-100 as an adsorbent for tetracycline removal from aqueous solution, *Environ. Sci. Pollut. Res.*, 29 (2022) 55026–55038.
- [27] Y. Li, Q. Du, T. Liu, Y. Qi, P. Zhang, Z. Wang, Y. Xia, Preparation of activated carbon from *Enteromorpha prolifera* and its use on cationic red X-GRL removal, *Appl. Surf. Sci.*, 257 (2011) 10621–10627.
- [28] M. Li, Y. Li, X. Zhang, H. Zheng, A. Zhang, T. Chen, W. Liu, Y. Yu, J. Liu, Q. Du, D. Wang, Y. Xia, One-step generation of S and N co-doped reduced graphene oxide for high-efficiency adsorption towards methylene blue, *RSC Adv.*, 10 (2020) 37757–37765.
- [29] Q. Liao, H. Rong, M. Zhao, H. Luo, Z. Chu, R. Wang, Strong adsorption properties and mechanism of action with regard to tetracycline adsorption of double-network polyvinyl alcohol-copper alginate gel beads, *J. Hazard. Mater.*, 422 (2022) 126863, doi: 10.1016/j.jhazmat.2021.126863.
- [30] J. Zhou, K. Zhu, Y. Wang, P. Cui, L. Zhu, H. Wu, M. Hua, Y. Huang, G. Luo, Y. Chao, W. Zhu, Facile hydrothermal synthesis of Cu<sub>2</sub>MoS<sub>4</sub> and FeMoS<sub>4</sub> for efficient adsorption of chlortetracycline, *Catalysts*, 13 (2023) 61, doi: 10.3390/catal13010061.
- [31] X. Wang, B. Cheng, L. Zhang, J. Yu, Y. Li, Synthesis of MgNiCo LDH hollow structure derived from ZIF-67 as superb adsorbent for Congo red, *J. Colloid Interface Sci.*, 612 (2022) 598–607.
- [32] Y. Guo, C. Yan, P. Wang, L. Rao, C. Wang, Doping of carbon into boron nitride to get the increased adsorption ability for tetracycline from water by changing the pH of solution, *Chem. Eng. J.*, 387 (2020) 124136, doi: 10.1016/j.cej.2020.124136.
- [33] L. Jin, X. Amaya-Mazo, M.E. Apel, S.S. Sankisa, E. Johnson, M.A. Zbyszynska, A. Han, Ca<sup>2+</sup> and Mg<sup>2+</sup> bind tetracycline with distinct stoichiometries and linked deprotonation, *Biophys. Chem.*, 128 (2007) 185–196.
- [34] K. Hemmat, M.R. Khodabakhshi, A. Zeraatkar Moghaddam, Synthesis of nanoscale zero-valent iron modified graphene oxide nanosheets and its application for removing tetracycline

- antibiotic: response surface methodology, *Appl. Organomet. Chem.*, 35 (2021) e6059, doi: 10.1002/aoc.6059.
- [35] A. Paula Fagundes, A. Felipe Viana da Silva, B. Bueno de Morais, D. Lusitâneo Pier Macuvele, J. Nones, H. Gracher Riella, N. Padoin, C. Soares, A novel application of bentonite modified with copper ions in the tetracycline adsorption: an experimental design study, *Mater. Lett.*, 291 (2021) 129552, doi: 10.1016/j.matlet.2021.129552.
- [36] Y. Kong, K. Han, Y. Zhuang, B. Shi, Facile synthesis of MOFs-templated carbon aerogels with enhanced tetracycline adsorption performance, *Water*, 14 (2022) 504, doi: 10.3390/w14030504.
- [37] Y. Zhang, Y. Li, W. Xu, M. Cui, M. Wang, B. Chen, Y. Sun, K. Chen, L. Li, Q. Du, X. Pi, Y. Wang, Filtration and adsorption of tetracycline in aqueous solution by copper alginate-carbon nanotubes membrane which has the muscle-skeleton structure, *Chem. Eng. Res. Des.*, 183 (2022) 424–438.
- [38] X. Mi, M. Wang, F. Zhou, X. Chai, W. Wang, F. Zhang, S. Meng, Y. Shang, W. Zhao, G. Li, Preparation of La-modified magnetic composite for enhanced adsorptive removal of tetracycline, *Environ. Sci. Pollut. Res.*, 24 (2017) 17127–17135.
- [39] W. Wang, M. Gao, M. Cao, J. Dan, H. Yang, Self-propagating synthesis of Zn-loaded biochar for tetracycline elimination, *Sci. Total Environ.*, 759 (2021) 143542, doi: 10.1016/j.scitotenv.2020.143542.
- [40] Y. Ma, M. Li, P. Li, L. Yang, L. Wu, F. Gao, X. Qi, Z. Zhang, Hydrothermal synthesis of magnetic sludge biochar for tetracycline and ciprofloxacin adsorptive removal, *Bioresour. Technol.*, 319 (2021) 124199, doi: 10.1016/j.biortech.2020.124199.
- [41] G. Sharma, S. Bhogal, A. Kumar, Mu. Naushad, S. Sharma, T. Ahamad, F.J. Stadler, AgO/MgO/FeO@Si<sub>3</sub>N<sub>4</sub> nanocomposite with robust adsorption capacity for tetracycline antibiotic removal from aqueous system, *Adv. Powder Technol.*, 31 (2020) 4310–4318.
- [42] S. Biniak, G. Szymański, J. Siedlewski, A. Świątkowski, The characterization of activated carbons with oxygen and nitrogen surface groups, *Carbon*, 35 (1997) 1799–1810.
- [43] Z. Yan, L. Liu, Y. Zhang, J. Liang, J. Wang, Z. Zhang, X. Wang, Activated semi-coke in SO<sub>2</sub> removal from flue gas: selection of activation methodology and desulfurization mechanism study, *Energy Fuels*, 27 (2013) 3080–3089.
- [44] N. Chubar, V. Gerda, D. Banerjee, G. Yablokova, Effect of Fe(II)/Ce(III) dosage ratio on the structure and anion adsorptive removal of hydrothermally precipitated composites: insights from EXAFS/XANES, XRD and FT-IR, *J. Colloid Interface Sci.*, 487 (2017) 388–400.
- [45] J. Shangguan, C. Li, M. Miao, Z. Yang, Surface characterization and SO<sub>2</sub> removal activity of activated semi-coke with heat treatment, *New Carbon Mater.*, 23 (2008) 37–43.
- [46] Z. Zhang, H. Liu, L. Wu, H. Lan, J. Qu, Preparation of amino-Fe(III) functionalized mesoporous silica for synergistic adsorption of tetracycline and copper, *Chemosphere*, 138 (2015) 625–632.
- [47] J. Yang, S. Ren, T. Zhang, Z. Su, H. Long, M. Kong, L. Yao, Iron doped effects on active sites formation over activated carbon supported Mn-Ce oxide catalysts for low-temperature SCR of NO, *Chem. Eng. J.*, 379 (2020) 122398, doi: 10.1016/j.cej.2019.122398.
- [48] S. Li, W. Huang, P. Yang, Z. Li, B. Xia, M. Li, C. Xue, D. Liu, One-pot synthesis of N-doped carbon intercalated molybdenum disulfide nanohybrid for enhanced adsorption of tetracycline from aqueous solutions, *Sci. Total Environ.*, 754 (2021) 141925, doi: 10.1016/j.scitotenv.2020.141925.
- [49] S. Zhu, P. Zhang, J. Zhang, X. Song, Y. Wang, X. Wang, J. Liu, B. Sun, Efficient adsorption of tetracycline in water by Mn and Ce codoped MIL-100 composite oxide, *Desal. Water Treat.*, 283 (2023) 185–195.
- [50] B. Sun, H. Zhou, J. Zhang, A. Hu, J. Mao, Y. Wang, X. Wang, S. Zhu, Preparation and characterization of a spherical Cu/Mn/Ce ternary nanocomposite oxide with high adsorption efficiency of tetracycline, *Desal. Water Treat.*, 264 (2022) 270–279.
- [51] S. Sun, Z. Yang, J. Cao, Y. Wang, W. Xiong, Copper-doped ZIF-8 with high adsorption performance for removal of tetracycline from aqueous solution, *J. Solid State Chem.*, 285 (2020) 121219, doi: 10.1016/j.jssc.2020.121219.
- [52] J. Tang, Y. Ma, C. Zeng, L. Yang, S. Cui, S. Zhi, F. Yang, Y. Ding, K. Zhang, Z. Zhang, Fe-Al bimetallic oxides functionalized-biochar via ball milling for enhanced adsorption of tetracycline in water, *Bioresour. Technol.*, 369 (2023) 128385, doi: 10.1016/j.biortech.2022.128385.